Fashion and Textiles

RESEARCH Open Access

Improved flame retardancy and mechanical properties of bacterial cellulose fabrics via solvent exchange and entrapment of zein and gluten

Hyunjin Kim[1] and Hye Rim Kim[2*]

*Correspondence:
khyerim@sookmyung.ac.kr

[1] Textile Innovation R&D Department, Smart Textronics Center, Korea Institute of Industrial Technology, 143 Hanggaul-ro, Sangrok-gu, Ansan-si, Gyeonggi-do 15588, South Korea
[2] Department of Clothing and Textiles, Sookmyung Women's University, Cheongpa-ro 47-Gil 100, Yongsan-gu, Seoul 04310, South Korea

Abstract

This study aimed to improve the flame retardancy and mechanical properties of bacterial cellulose (BC) by introducing cereal proteins, namely zein and gluten. The production conditions were determined by observing residual masses of samples at 1000 ℃ using thermogravimetric analysis (TGA). According to the TGA results, the optimized production conditions for the BCs with zein and gluten were combined solvent exchange and entrapment of 20 weight% (wt.%) of zein, and entrapment of 40 wt.% of gluten, respectively. Surface characterization of BC prepared with zein and gluten under the optimal conditions confirmed that the cereal proteins were incorporated into the BC nanostructures via solvent exchange and/or entrapment and the original chemical and crystal structures of BC were not significantly changed. Limiting oxygen index (LOI) analysis confirmed that cereal proteins improved the flame retardancy of BC. In particular, the LOI of BC entrapped with gluten was 50%, which was better than that of cowhide leather. Char morphology analysis confirmed that the as-produced BCs with cereal proteins exhibited condensed-phase flame-retardant mechanism by forming intumescent chars. Analysis of the mechanical properties confirmed that compared with cowhide leather, as-produced BCs with cereal proteins possessed high tensile strength and dimensional stability, making them suitable leather substitutes.

Keywords: Bacterial cellulose, Flame retardancy, Zein, Gluten, Entrapment, Mechanical property

Introduction

Bacterial cellulose (BC) is an environmentally-friendly cellulosic material produced by *Gluconacetobacter xylinus* and *Acetobacter xylinus* (Kim et al., 2020). BC has received attention as a sustainable fabric because the appearance of dry BC is similar to that of natural leather, and it also has excellent moldability and a controllable shape (Kim et al., 2021a). However, BC is highly combustible due to its cellulosic structure (Kim & Kim, 2023); thus, the flammability of BC may restrict its application as a natural leather substitute. Thus, to expand the application of BC, flame-retardant finishing is needed.

In this study, cereal proteins (zein and gluten) obtained from the agricultural and biofuel industries are selected as additives to impart flame retardancy to BC. Because these proteins are biomass materials, their utilization would reduce waste generation (Peydayesh et al., 2023). Zein is a corn storage protein with good biodegradability and barrier properties (Gonçalves et al., 2020; Yang et al., 2020). Gluten is a wheat protein with good thermal stability because of its high sulfur content (Yuan et al., 2010).

Therefore, the first aim of this study was to produce BC with enhanced flame retardancy using zein and gluten, which are inexpensive biomass raw materials. However, cereal proteins have poor solubility in water (Kasaai, 2018), making them difficult to incorporate into BC. Thus, the second aim of this study was to introduce methods of finishing BC using cereal proteins; this was achieved via solvent exchange and entrapment methods. The solvent exchange involves replacing the solvent in a compound while maintaining the dissolved molecules in the solution (Fazlollahi & Wankat, 2018). Entrapment involves physically enclosing molecules inside BC without changing its nanostructure (Kim & Kim, 2023). The solvent exchange and entrapment methods are both very simple and easily implemented, which shortens the fabrication process.

The novelty of this study lay in improving the flame retardancy and mechanical properties of BC using inexpensive and eco-friendly biomass materials through simple methods. After producing BCs with cereal proteins under optimized conditions, the surface characterization, flame retardancy, and mechanical properties are analyzed.

Experimental

Materials

Glucose, hydrogen peroxide (H_2O_2; 34.5%), sodium hydroxide (NaOH; pellets), and 1 N NaOH solution were obtained from Duksan Pure Chemicals (Ansan, South Korea), and a kombucha symbiotic culture of bacteria and yeast (SCOBY) was purchased from Getkombucha (Broomfield, CO, USA). Yeast extract and peptone were obtained from BD Biosciences (San Jose, CA, USA). Zein from corn, wheat gluten, and sodium dodecylbenzenesulfonate ($C_{18}N_{29}NaO_3S$; SDBS) were supplied by Sigma-Aldrich (St. Louis, MO, USA). All the reagents were used as received without further purification. Untanned raw cowhide leather scrap was obtained from a local leather shop in South Korea. The thickness of the scraps was 0.7 ± 0.4 mm, which was similar to that of the BC samples.

Production and pretreatments of original BC

BC was produced by acetic acid bacteria within the kombucha SCOBY and was subjected to pretreatments including washing, bleaching, and swelling (Han et al., 2019; Song et al., 2017). The pre-treated BC is denoted as 'original BC.'

Production of BCs with cereal proteins

Herein, the BC sample produced via combined solvent exchange and entrapment using zein is denoted as 'BC-zein-SE,' and the BC sample produced by gluten entrapment is named as 'BC-gluten-E'. BC-zein-SE was produced based on the method described by Wan et al. (2017) with some modifications. Briefly, original BC (wet state) was immersed in an 80% (v/v) ethanol solution at 25 ℃ for 24 h for solvent exchange of water to ethanol inside original BC. Subsequently, a zein solution was prepared by dissolving zein

powder in a range of 0–60 wt.% relative to original BC in an 80% (v/v) ethanol solution at a BC:liquor ratio of 1:10 (w/v), and was ultrasonicated at 25 ℃ for 30 min. Thereafter, solvent-exchanged BC was immersed in the zein solution, followed by ultrasonication at 25 ℃ for 30 min, shaking at 80 rpm for 1 h in a shaking water bath at 30 ℃, and drying in a drying oven (OF-22G, JEIO TECH Co., Daejeon, South Korea) at 25 ℃ for 24 h to obtain BC-zein-SE. BC-gluten-E was produced based on the method of Kim et al. (2021b) with some modifications; an alkaline NaOH solution was used to dissolve gluten powders (Mathew et al., 2019). Briefly, a gluten solution was prepared by dissolving gluten powder in the range of 0–60 wt.% relative to original BC in NaOH solution (0.25 M) at a BC:liquor ratio of 1:10 (w/v), and was ultrasonicated at 25 ℃ for 30 min. Thereafter, the gluten solution was denatured at 80 ℃ for 20 min with shaking at 80 rpm in a shaking water bath and cooled to 25 ± 2 ℃. Original BC was then immersed in the solution, followed by ultrasonication at 25 ℃ for 30 min, shaking at 80 rpm for 1 h in a shaking water bath at 30 ℃, and drying in a drying oven at 25 ℃ for 24 h to obtain BC-gluten-E.

Characterization of BCs with cereal proteins

The FT-IR spectra of the samples were recorded using a Nicolet iS50 FT-IR spectrometer (Thermo Fisher Scientific, Waltham, MA, USA). Each spectrum was baseline-normalized using the OMNIC program (Thermo Fisher Scientific, Waltham, MA, USA). XRD patterns of the samples were acquired using a D8 ADVANCE X-ray diffractometer (Bruker, Billerica, MA, USA) with a Cu-Kα radiation source (λ = 0.15418 nm). The DIFFRAC.SUITE™ program (Bruker, Billerica, MA, USA) was used to perform background subtraction and smoothing. The degree of crystallinity is calculated as follows (Eq. 1):

$$\text{Degree of crystallinity (\%)} = \left| \frac{A_{\text{cryst}}}{A_{\text{total}}} \right| \times 100 \quad (1)$$

where A_{cryst} is the sum of the crystalline band areas and A_{total} is the total area under the diffractogram (Adepu & Khandelwal, 2021). The surface and cross-sectional morphologies of samples were evaluated using a FE-SEM instrument (JSM-7800F, Prime, JEOL, Tokyo, Japan). All samples were sputter-coated with Pt using a magnetron sputter-coater (108auto, Cressington Scientific Instruments, Watford, UK). Along with FE-SEM, EDX was used to detect C, O, N, P, and S on the surface of the samples.

Flame-retardant properties of BCs with cereal proteins

To determine the residual masses of samples at 1000 ℃, thermogravimetric analysis (TGA) was performed at a heating rate of 10 ℃/min under N_2 atmosphere (flow rate of 60 mL/min) using a thermal analyzer (Discovery SDT 650, TGA Instruments, New Castle, DE, USA).

The LOI of each sample was measured using a LOI instrument (Fire Testing Technology, West Sussex, UK) according to the ISO 4589-2:2017 standard (Plastics—Determination of burning behavior of oxygen index—Part 2: Ambient temperature test). The dimensions of each sample were 80 mm × 10 mm × 1 mm.

The char residues obtained after combustion were analyzed at 100× and 1000× magnifications using an FE-SEM instrument (SU-3500, Hitachi, Ltd., Tokyo, Japan).

Mechanical property analyses of BCs with cereal proteins

The tensile strength and elongation of the samples were examined according to the ASTM D882-18 standard (Standard Test Method for Tensile Properties of Thin Plastic Sheeting) using a universal testing machine (HZ-1007A, Dongguan Lixian Instrument Scientific, Dongguan, China).

The softness of each sample was evaluated according to the ISO 17235:2015 standard (Leather—Physical and mechanical tests—Determination of softness) using a digital leather softness tester (XB-OTS-TF115, Dongguan Xinbao Instrument, Dongguan, China). The crease recovery angles of the samples were measured according to the ISO 2313:1972 standard (Textiles—Determination of the Recovery from Creasing a Horizontally Folded Specimen of Fabric by Measuring the Angle of Recovery).

The dimensional stability of the samples was evaluated according to the ISO 7771:1985 standard (Textiles—Determination of Dimensional Changes of Fabrics Induced by Cold-Water Immersion) with slight modifications. The size of each sample was 50 × 100 mm, and the duration of the study was 60–180 min.

Results and Discussion

Conditions for producing BCs with cereal proteins

Optimization of conditions for producing BCs with cereal proteins

Generally, a higher residual mass of a sample after thermogravimetric analysis (TGA) is attributed to greater char formation (Zhu et al., 2004). Hence, the optimal conditions for producing BC using cereal proteins were determined based on the residual mass data collected from TGA at 1000 ℃.

As shown in Fig. 1, the residual masses of BC-zein-SE and BC-gluten-E (see Experimental) increased as the amounts of zein and gluten increased, and were highest with the incorporation of 20 and 40 wt.% of zein and gluten relative to BC, respectively. However, when zein and gluten contents exceeded the highest value, the residual masses of BC-zein-SE and BC-gluten-E decreased. As the amounts of cereal proteins increased,

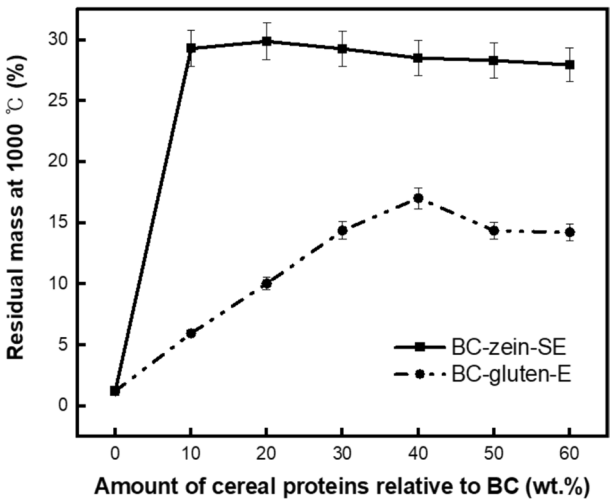

Fig. 1 Residual masses at 1000 ℃ of BC-zein-SE and BC-gluten-E produced with different amounts of zein and gluten

fewer hydroxyl groups in BC would be available for reaction (Liu et al., 2019). Hence, the excess protein molecules were aggregated on the surface of BC, thereby decreasing the thermal stability (Wang et al., 2016). Therefore, the optimal conditions for producing BCs with cereal proteins were as follows: (1) Production conditions for BC-zein-SE: combined solvent exchange and entrapment, 80% (v/v) ethanol–water solution, immersion for 24 h, and 20 wt.% zein relative to BC; (2) Production conditions of BC-gluten-E: entrapment, 0.25 M NaOH solution, 40 wt.% gluten relative to BC.

Characterization of BCs with cereal proteins

FT-IR analysis

FT-IR spectroscopy was used to examine the chemical interactions between BC and cereal proteins. The FT-IR spectra of all samples (Fig. 2) show characteristic peaks of BC at 3300–3500, 2920–2960, 1054, and 1030 cm^{-1}, confirming that the chemical structure of BC remained unchanged after entrapping cereal proteins (Kim & Kim, 2023). Moreover, the O–H stretching peak in the FT-IR spectrum of the original BC was shifted to lower wavenumbers after protein entrapment. The blue shifts may originate from

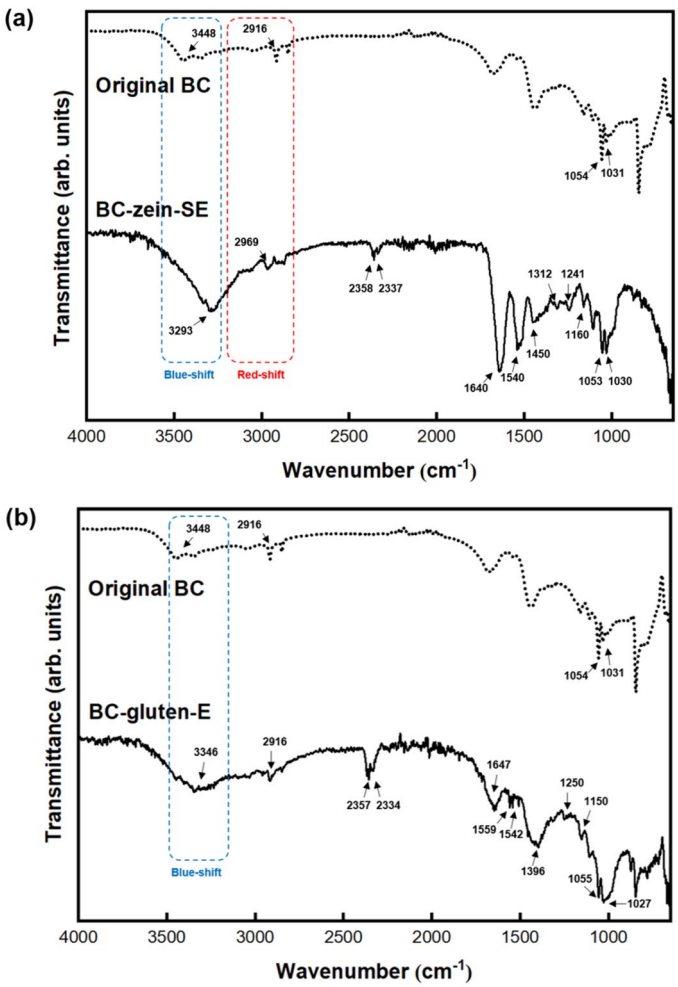

Fig. 2 FT-IR spectra of **a** original BC and BC-zein-SE, and **b** original BC and BC-gluten-E

hydrogen bond formation, indicating a chemical interaction between BC and cereal proteins (Lee et al., 2015). Conversely, a shift to a higher wavenumber was observed for the C–H stretching peak in the FT-IR spectrum of BC-zein-SE. The red shift is attributed to the loose hydrogen bonds between BC and zein (Kudo & Nakashima, 2020), suggesting that compared with zein, gluten is more strongly bound to BC. The FT-IR spectra of BC-zein-SE and BC-gluten-E show typical absorption bands of proteins in the amide I (1600–1700 cm^{-1}), amide II (1500–1600 cm^{-1}), and amide III (1240–1450 cm^{-1}) regions, suggesting that the cereal proteins were entrapped within BC (Mejia et al., 2007; Peng et al., 2022; Xie et al., 2020; Zhang et al., 2022). Furthermore, the new peaks at 2330–2360 cm^{-1} and 1150–1160 cm^{-1} in the FT-IR spectra of BC-zein-SE and BC-gluten-E also indicate the presence of zein and gluten within BC, respectively (Avila et al., 2020; Hosseini et al., 2022; Mohammadia et al., 2018). Thus, it was confirmed that the cereal proteins formed hydrogen bonds with BC and the chemical structure of BC was retained after entrapping cereal proteins.

XRD analysis

XRD was used to analyze the crystalline structures of BCs with cereal proteins. The diffraction pattern of the original BC (Fig. 3) shows peaks at $2\theta = 14.8°$, 17.2°, 23.0°,

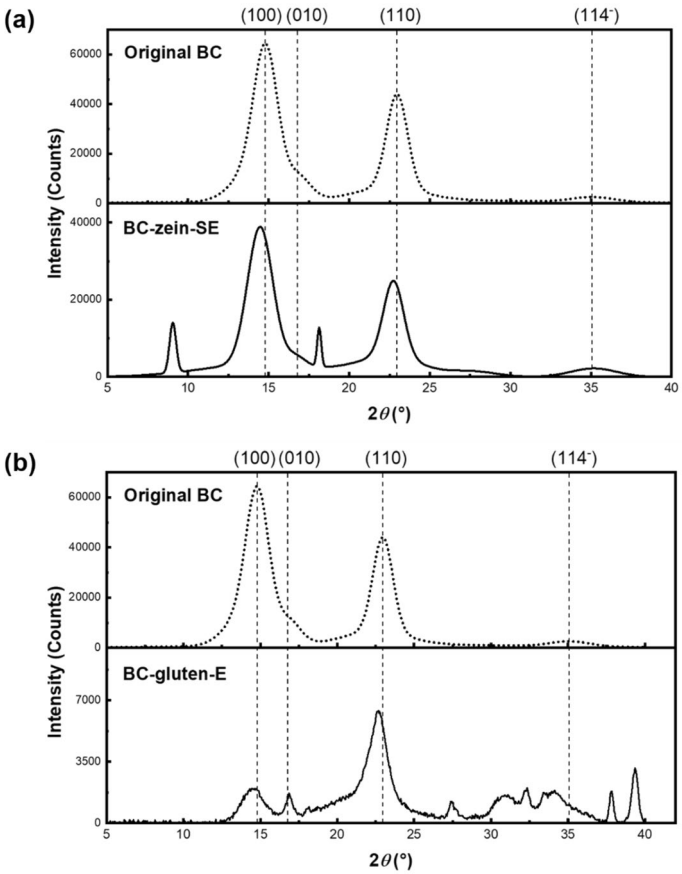

Fig. 3 XRD patterns of **a** original BC and BC-zein-SE, and **b** original BC and BC-gluten-E

and 34.1°, indicating the cellulose Iα structure (French, 2014). These peaks were also observed in the diffraction patterns of BC-zein-SE and BC-gluten-E, confirming that the entrapment of cereal proteins did not change the crystal structure of BC. In the diffraction pattern of BC-zein-SE, new peaks appeared at $2\theta = 9.0°$ and 18.5°, corresponding to the α-helix and β-sheet structures of zein, respectively (Martelli-Tosi et al., 2018). Moreover, a new peak also appeared at $2\theta = 27.3°$, which might be attributed to the ionic interaction between zein and BC (Xu et al., 2022). In the diffraction pattern of BC-gluten-E, new peaks appeared at $2\theta = 27.3°$, 30.9°, 32.2°, and 39.4°, which might reflect the intermolecular interaction between gluten and BC (Abugoch et al., 2011). The diffraction pattern of BC-gluten-E also showed a peak at $2\theta = 37.8°$, corresponding to the crystalline domain of gliadin (Rani et al., 2021). Hence, it was confirmed that zein and gluten were entrapped within BC. Moreover, the crystallinity of BC increased from 85.1% to 92.7% and 87.7% after entrapping zein and gluten, respectively. The self-assembly nature of cereal proteins can increase the strength of hydrogen bonding between BC and proteins, thereby forming better-packed structures, leading to increased crystallinity (Keshk & Sameshima, 2006; Poletto et al., 2012).

SEM analysis

The surface morphology of BCs with cereal proteins was examined (Fig. 4). The SEM images of the original BC show interlaced cellulose nanofibers. The SEM images of BC-zein-SE show dense structures with spherical zein particles aggregated on the surface. The aggregation of zein may result from the noncovalent interactions with BC (Ding et al., 2022). In the SEM images of BC-gluten-E show thickened BC fibers, where the spaces between the fibers were filled, which might be attributed to the entrapped gluten (Lin et al., 2009). The cross-sectional SEM image of the original BC

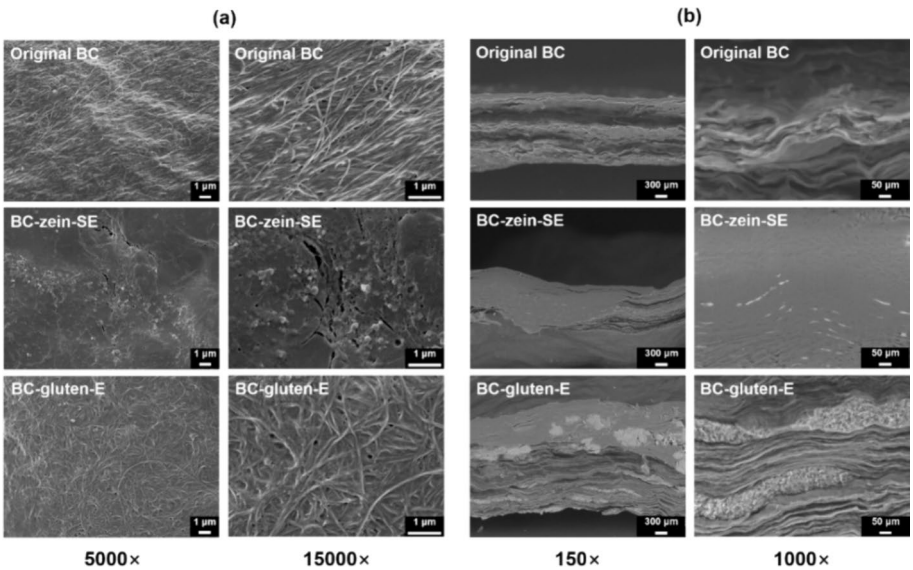

Fig. 4 SEM images of **a** the surface morphologies of original BC, BC-zein-SE, and BC-gluten-E at 5000× and 15000× magnifications, respectively, and **b** the cross-sections of original BC, BC-zein-SE, and BC-gluten-E at 150× and 1000× magnifications, respectively

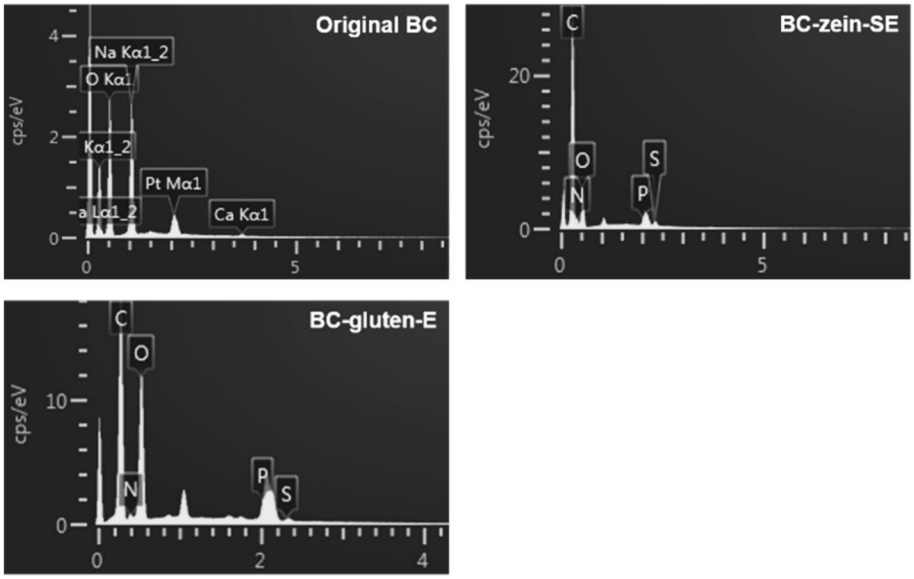

Fig. 5 EDX spectra of original BC, BC-zein-SE, and BC-gluten-E

Table 1 Surface elemental compositions of original BC, BC-zein-SE, and BC-gluten-E

Sample	Surface elemental compositions (wt.%)				
	C	O	N	P	S
Original BC	48.74	40.79	-	-	-
BC-zein-SE	65.96	24.22	9.29	0.05	0.48
BC-gluten-E	55.38	39.85	3.41	-	1.37

C: Carbon; O: Oxygen; N: Nitrogen; P: Phosphorus; S: Sulphur

shows a multilayered structure formed through the layer-by-layer assembly of BC sheets during cultivation (Jiamsawat et al., 2022). The cross-sectional SEM images of BC-zein-SE and BC-gluten-E show densely packed structures, which might influence the tensile strength of the composites (Jebel & Almasi, 2016).

EDX analysis

EDX was used to analyze the surface elemental compositions of samples. C and O, which are the major elements constituting BC fibers, were found in the EDX spectra of all samples (Fig. 5 and Table 1). This observation is consistent with the unchanged chemical structure of BC (Villarreal-Soto et al., 2020). N and S, which are typical elements of proteins, were observed in the EDX spectra of BC-zein-SE and BC-gluten-E. The presence of these elements confirms the entrapment of cereal proteins (Ahmed & Rehman, 2020; Chen et al., 2022). In addition, P was detected only in the EDX spectrum of BC-zein-SE because of the different elemental compositions of zein and gluten; zein is mainly composed of N, P, and S, whereas gluten is mainly composed of N and S (Ahmed & Rehman, 2020; Chen et al., 2022).

Flame-retardant properties of BCs with cereal proteins

TGA analysis

The TGA curve of the original BC shows four mass-loss stages (Fig. 6). During the first degradation stage (≤ 200 ℃), the mass loss of the original BC is owing to the evaporation of water (Sheykhnazari et al., 2018). During the second (200–350 ℃) and third (350–570 ℃) stages, the mass loss of the original BC is due to the volatilization of BC (Kiziltas et al., 2015). In the fourth stage (570–1000 ℃), the original BC was finally decomposed to ash (Abral et al., 2020). The TGA curve of BC-zein-SE comprised two degradation stages. During the first degradation stage (≤ 400 ℃), the mass loss of BC-zein-SE is due to the major degradation of zein (Altan et al., 2018). The mass loss of BC-zein-SE in the second stage (400–1000 ℃) corresponds to carbonization (Ghorbani et al., 2020). By contrast, the TGA curve of BC-gluten-E showed four degradation stages. The first stage (≤ 190 ℃) corresponds to moisture loss from both BC and gluten (Khatkar et al., 2013). The second stage of mass loss (190–330 ℃) for BC-gluten-E is attributed to the thermal decomposition of the cellulose structure (Chong et al., 2019). During the third stage (330–550 ℃), gluten underwent chain breakage and volatilization (Peng et al., 2021). During the final degradation stage (550–1000 ℃), the mass loss of BC-gluten-E corresponds to the thermal decomposition of the char residue (Liu et al., 2020). The char residues of BC-zein-SE and BC-gluten-E at 1000 ℃ accounted for 29.890 and 17.048% of their initial masses, respectively. Because char residues can protect BC from combustion (Zhang et al., 2018), the results confirmed that the thermal stability of BC was improved after the entrapment of cereal proteins.

LOI analysis

The LOI experiment was held to determine the flame retardancy of the samples. The LOI of the original BC was 19%, which is similar to that of cotton (approximately 18%), indicating that original BC is a flammable material (Kim & Kim, 2023). The LOIs of BC-zein-SE and BC-gluten-E were 25% and 50%, respectively, which are similar to the literature data (Baishya et al., 2017; Kambli et al., 2018). The increase in the LOIs of BC-zein-SE

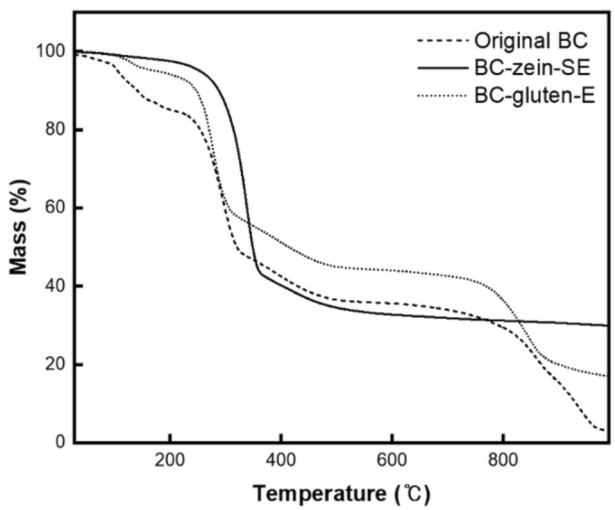

Fig. 6 TGA curves of original BC, BC-zein-SE, and BC-gluten-E

and BC-gluten-E may be attributed to the synergistic effects of P–N and S–N, respectively, in the flame-retardant system of cereal proteins (Chang et al., 2017). In particular, the LOI of BC-gluten-E was considerably higher than that of cowhide leather (30%). The high LOI of BC-gluten-E may be attributed to the different oxygen barrier properties of zein and gluten. The oxygen permeability of gluten is relatively low due to the intramolecular self-crosslinking of gluten, whereas that of zein is relatively high owing to its helical conformation (Tang et al., 2012). Therefore, the LOI results confirmed that the entrapment of cereal proteins improved the flame retardancy of BC and that gluten has relatively better flame retardancy than zein.

Char morphology analysis

The char morphologies were observed to analyze the mechanism underlying the flame retardancy of the samples. The char residues of the original BC have a fractured morphology (Fig. 7), indicating insufficient char formation (Ao et al., 2020). This char cannot inhibit the heat and mass transfer during combustion, resulting in poor flame resistance (Xu et al., 2020). The char residues of BC-zein-SE exhibited sponge-like structures, whereas those of BC-gluten-E comprised swollen bubbles. These two structures are the common structures of intumescent char, which can act as an insulating barrier that hinders flame propagation and heat and mass transfer during combustion (Das et al., 2020). Moreover, the bubbles observed in the char residues of BC- gluten-E are carbon bubbles created by nonflammable gases, such as oxygen (Li et al., 2011). Thus, it was confirmed that the entrapment of cereal proteins involved a condensed-phase flame-retardant mechanism, forming intumescent chars on the surface of BC.

Analyses of mechanical properties of BCs with cereal proteins

Tensile strength and elongation at break

As shown in Fig. 8a, the tensile strengths of BC-zein-SE and BC-gluten-E were significantly higher than that of the original BC. This can be explained by the effective stress transfer between BC and cereal proteins via interfacial adhesion (Li et al., 2020). Moreover, the densely packed structures of BC-zein-SE and BC-gluten-E (Fig. 4) might improve their tensile strengths (Jebel & Almasi, 2016). The tensile strengths of BC-zein-SE and BC-gluten-E were higher than those of cowhide leather. However, the elongation at break of BC-zein-SE and BC-gluten-E were similar to that of the original BC and were lower than that of cowhide leather (Fig. 8b). The strong hydrogen bonds between BC and cereal proteins may increase the rigidity of BC by restricting the movement of protein chains (Wang et al., 2017), thereby making BC less flexible and leading to early fracture (Wan et al., 2017).

Fabric softness and crease recovery

The fabric softness and crease recovery of samples were analyzed (Fig. 9), showing that the softness and crease resistance of BC-zein-SE and BC-gluten-E increased compared to those of the original BC, but were not better than those of cowhide leather. Typically, cellulosic fabrics exhibit poor crease resistance owing to the numerous free hydroxyl groups in their structure (Nallathambi et al., 2011). During creasing, cellulose chain slippage in the amorphous region causes hydrogen bonds to break and shift to new regions,

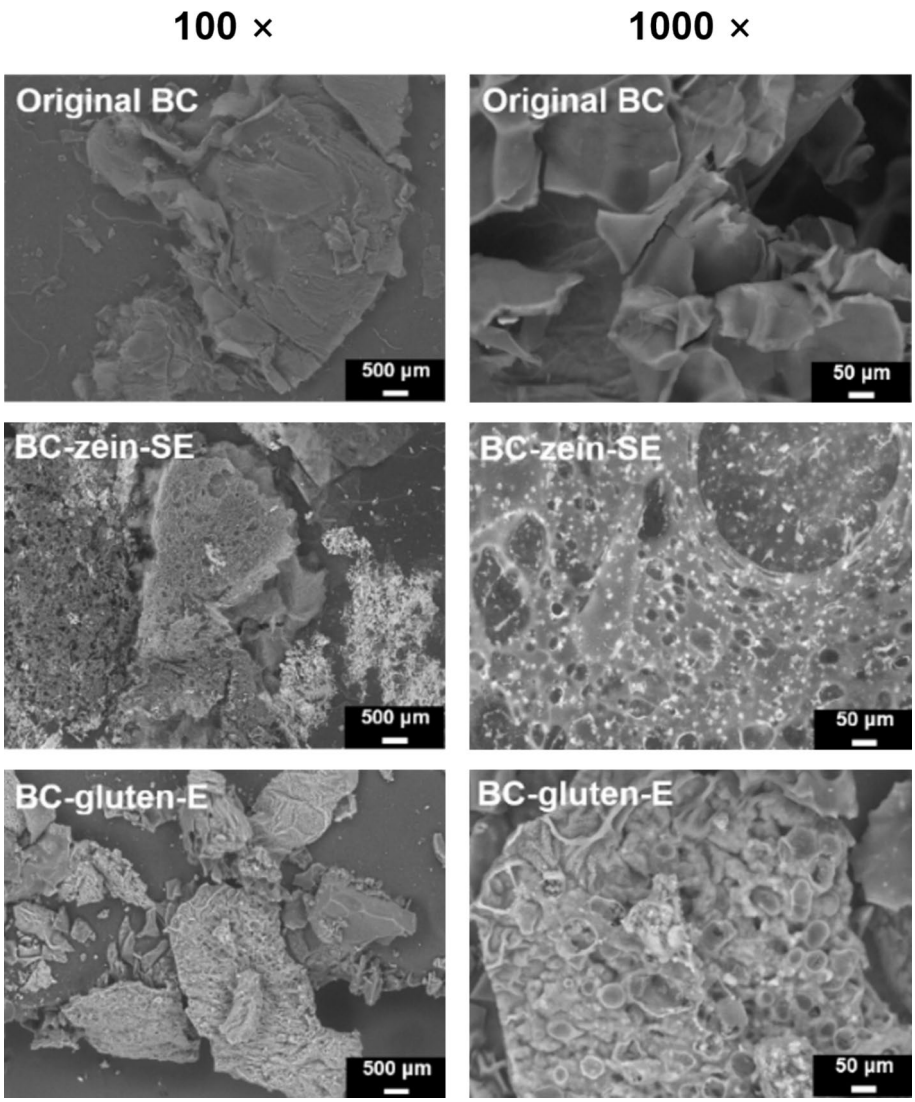

Fig. 7 Char morphologies of original BC, BC-zein-SE, and BC-gluten-E at 100× and 1000× magnifications, respectively

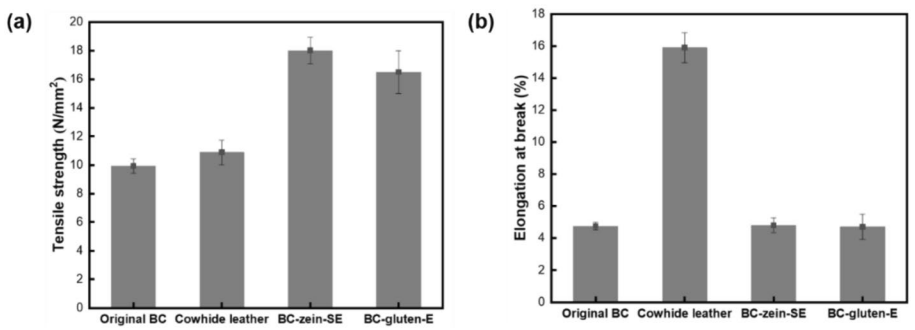

Fig. 8 **a** Tensile strengths and **b** elongations at break of original BC, cowhide leather, BC-zein-SE, and BC-gluten-E

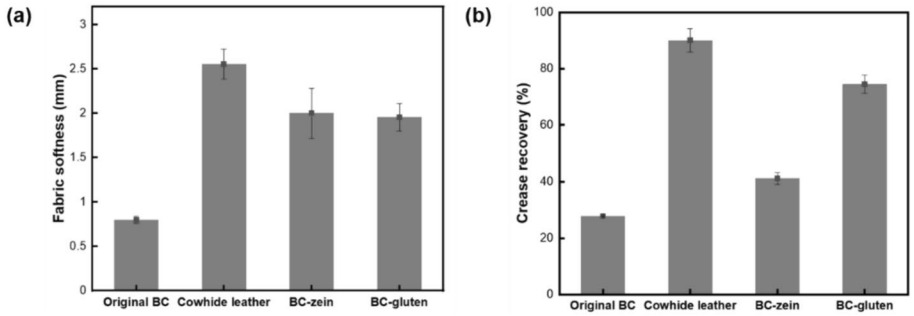

Fig. 9 **a** Fabric softness and **b** crease recovery of original BC, cowhide leather, BC-zein-SE, and BC-gluten-E

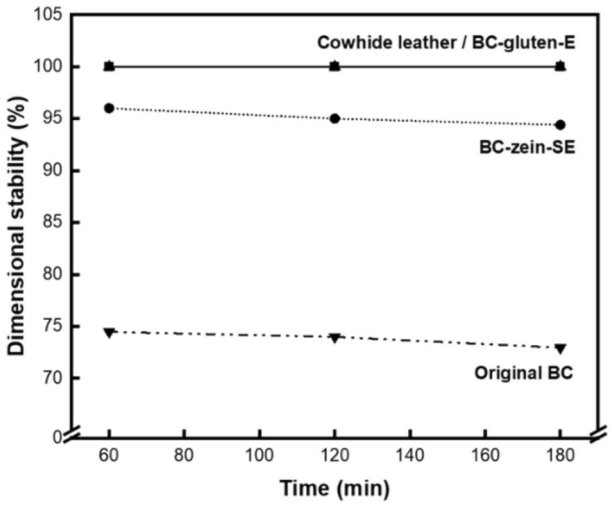

Fig. 10 Dimensional stabilities of original BC, cowhide leather, BC-zein-SE, and BC-gluten-E

increasing the rigidity and wrinkles (Chen et al., 2004; Raza et al., 2018; Tariq et al., 2022). However, if the hydroxyl groups of BC interact with protein molecules by forming hydrogen bonds, the stiffness of BC would be reduced by changing the BC fibril network through intermolecular interactions, thereby enhancing the crease resistance and softness (Barbi et al., 2021; Chen et al., 2018; Nallathambi et al., 2011).

Dimensional stability

The dimensional stability of the original BC was approximately 73–74% after immersion in the wetting solution for 180 min (Fig. 10). This is plausibly attributed to the aggregation of the BC fibers after the evaporation of water, which caused wrinkles on the surface (Domskiene et al., 2019). The dimensional stabilities of BC-zein-SE and BC-gluten-E were markedly higher than that of the original BC because the polymer chains within BC-zein-SE and BC-gluten-E were less mobile owing to the intermolecular interactions of the cereal proteins (Wang et al., 2017). Moreover, the dimensional stabilities of BC-zein-SE and BC-gluten-E were comparable to that of cowhide leather. Therefore, the results confirmed that the entrapment of cereal proteins improved the dimensional stability of BC.

Conclusions

The objective of this study was to improve the flame retardancy and mechanical properties of BC by using cereal proteins. After producing BCs with cereal proteins under optimal conditions, surface characterization revealed that zein and gluten were incorporated into BC nanostructures via solvent exchange and/or entrapment without affecting the original chemical and crystal structures of BC. The thermal stability of BC was improved by incorporating cereal proteins, forming char residues that protect BC from combustion. The LOI analysis confirmed that entrapment of cereal proteins improved the flame retardancy of BC. In particular, the LOI of BC-gluten-E was much higher than that of cowhide leather (30%), indicating that BC-gluten-E has better flame retardancy than that of cowhide leather. Char morphology analysis confirmed that the condensed-phase flame-retardant mechanism was operative for BC-zein-SE and BC-gluten-E, involving the formation of intumescent chars. The mechanical property analyses confirmed that both BC-zein-SE and BC-gluten-E had good tensile strength but less flexibility due to their rigidity. The dimensional stabilities of BC-zein-SE and BC-gluten-E were comparable to that of cowhide leather.

Abbreviations

BC	Bacterial cellulose
LOI	Limiting oxygen index
SCOBY	Symbiotic culture of bacteria and yeast
BC-zein-SE	Bacterial cellulose sample produced via combined solvent exchange and entrapment using zein
BC-gluten-E	Bacterial cellulose sample produced via entrapment using gluten

Supplementary Information

The online version contains supplementary material available at https://doi.org/10.1186/s40691-024-00395-7.

Supplementary Material 1.

Acknowledgements

The authors would like to thank Editage (www.editage.co.kr) for English language editing. The IRB approval is not applicable since this manuscript does not involve any human subjects and/or human subjects' data.

Author contributions

HK performed data analysis and wrote the first draft of the manuscript. HRK designed and supervised the experiments and revised the manuscript. All the authors have read and approved the final version of the manuscript.

Funding

This work was supported by the National Research Foundation of Korea (NRF) grant funded by the Korean government (MSIT) (Grant Number NRF-2022R1A2B5B01002588).

Availability of data and materials

All data generated or analyzed during this study are included in this article.

Declarations

Ethics approval and consent to participate

Not applicable.

Competing interests

The authors declare that they have no competing interests.

Received: 20 January 2024 Accepted: 15 July 2024
Published online: 05 August 2024

References

Abral, H., Fajri, N., Mahardika, M., Handayani, D., Sugiarti, E., & Kim, H.-J. (2020). A simple strategy in enhancing moisture and thermal resistance and tensile properties of disintegrated bacterial cellulose nanopaper. *Journal of Materials Research and Technology, 9*(4), 8754–8765. https://doi.org/10.1016/j.jmrt.2020.06.023

Abugoch, L. E., Tapia, C., Villamán, M. C., Yazdani-Pedram, M., & Díaz-Dosque, M. (2011). Characterization of quinoa protein-chitosan blend edible films. *Food Hydrocolloids, 25*(5), 879–886. https://doi.org/10.1016/j.foodhyd.2010.08.008

Adepu, S., & Khandelwal, M. (2021). Drug release behaviour and mechanism from unmodified an in situ modified bacterial cellulose. *Proceedings of the Indian National Science Academy, 87*, 110–120. https://doi.org/10.1007/s43538-021-00012-x

Ahmed, Y., & Rehman, M. A. U. (2020). Improvement in the surface properties of stainless steel via zein/hydroxyapatite composite coatings for biomedical applications. *Surfaces and Interfaces, 20*, Article 100589. https://doi.org/10.1016/j.surfin.2020.100589

Altan, A., Aytac, Z., & Uyar, T. (2018). Carvacrol loaded electrospun fibrous films from zein and poly(lactic acid) for active food packaging. *Food Hydrocolloids, 81*, 48–59. https://doi.org/10.1016/j.foodhyd.2018.02.028

Ao, X., Du, Y., Yu, D., Wang, W., Yang, W., Sun, B., & Zhu, M. (2020). Synthesis, characterization of a DOPO-based polymeric flame retardant and its application in polyethylene terephthalate. *Progress in Natural Science: Materials International, 30*(2), 200–207. https://doi.org/10.1016/j.pnsc.2020.01.018

Avila, L. B., Fontes, M. R. V., da Rosa Zavareze, E., Moraes, C. C., Morais, M. M., & da Rosa, G. S. (2020). Recovery of bioactive compounds from Jaboticaba peels and application into zein ultrafine fibers produced by electrospinning. *Polymers, 12*(12), Article 2916. https://doi.org/10.3390/polym12122916

Baishya, P., Saikia, D., Mandal, M., & Maji, T. K. (2017). Biodegradability, flammability, dimensional stability, and UV resistance study of green wood starch gluten nanocomposites. *Polymer Composites, 40*(1), 46–55. https://doi.org/10.1002/pc.24598

Barbi, S., Taurino, C., La China, S., Anguluri, K., Gullo, M., & Montorsi, M. (2021). Mechanical and structural properties of environmental green composites based on functionalized bacterial cellulose. *Cellulose, 28*, 1431–1442. https://doi.org/10.1007/s10570-020-03602-y

Chang, S. C., Nguyen, M., Condon, B., & Smith, J. (2017). The comparison of phosphorus-nitrogen and sulfur-phosphorus-nitrogen on the anti-flammability and thermal degradation of cotton fabrics. *Fibers and Polymers, 18*, 666–674. https://doi.org/10.1007/s12221-017-6686-x

Chen, S.-Q., Lopez-Sanchez, P., Wang, D., Mikkelsen, D., & Gidley, M. J. (2018). Mechanical properties of bacterial cellulose synthesized by diverse strains of the genus *Komagataeibacter*. *Food Hydrocolloids, 81*, 87–95. https://doi.org/10.1016/j.foodhyd.2018.02.031

Chen, W., Lickfield, G. C., & Yang, C. Q. (2004). Molecular modeling of cellulose in amorphous state part II: Effects of rigid and flexible crosslinks on cellulose. *Polymer, 45*(21), 7357–7365. https://doi.org/10.1016/j.polymer.2004.08.023

Chen, Y., Li, Y., Qin, S., Han, S., & Qi, H. (2022). Antimicrobial, UV blocking, water-resistant and degradable coatings and packaging films based on wheat gluten and lignocellulose for food preservation. *Composites Part B: Engineering, 238*, Article 109868. https://doi.org/10.1016/j.compositesb.2022.109868

Chong, C. T., Mong, G. R., Ng, J.-H., Chong, W. W. F., Ani, F. N., Lam, S. S., & Ong, H. C. (2019). Pyrolysis characteristics and kinetic studies of horse manure using thermogravimetric analysis. *Energy Conversion and Management, 180*, 1260–1267. https://doi.org/10.1016/j.enconman.2018.11.071

Das, O., Kim, N. K., Hedenqvist, M. S., Bhattacharyya, D., Johansson, E., Xu, Q., & Holder, S. (2020). Naturally-occurring bromophenol to develop fire retardant gluten biopolymers. *Journal of Cleaner Production,243*, Article 118552. https://doi.org/10.1016/j.jclepro.2019.118552

Ding, Z., Chang, X., Fu, X., Kong, H., Yu, Y., Xu, H., Shan, Y., & Ding, S. (2022). Fabrication and characterization of pullulan-based composite films incorporated with bacterial cellulose and ferulic acid. *International Journal of Biological Macromolecules, 219*, 121–137. https://doi.org/10.1016/j.ijbiomac.2022.07.236

Domskiene, J., Sederaviciute, F., & Simonaityte, J. (2019). Kombucha bacterial cellulose for sustainable fashion. *International Journal of Clothing Science and Technology, 31*(5), 644–652. https://doi.org/10.1108/ijcst-02-2019-0010

Fazlollahi, F., & Wankat, P. C. (2018). Novel solvent exchange distillation column. *Chemical Engineering Science, 184*, 216–228. https://doi.org/10.1016/j.ces.2018.02.025

French, A. D. (2014). Idealized powder diffraction patterns for cellulose polymorphs. *Cellulose, 21*, 885–896. https://doi.org/10.1007/s10570-013-0030-4

Ghorbani, M., Nezhad-Mokhtari, P., & Ramazani, S. (2020). *Aloe vera*-loaded nanofibrous scaffold based on Zein/Polycaprolactone/Collagen for wound healing. *International Journal of Biological Macromolecules, 153*, 921–930. https://doi.org/10.1016/j.ijbiomac.2020.03.036

Gonçalves, J., Torres, N., Silva, S., Gonçalves, F., Noro, J., Cavaco-Paulo, A., Ribeiro, A., & Silva, C. (2020). Zein impart hydrophobic and antimicrobial properties to cotton textiles. *Reactive and Functional Polymers,154*, Article 104664. https://doi.org/10.1016/j.reactfunctpolym.2020.104664

Han, J., Shim, E., & Kim, H. R. (2019). Effects of cultivation, washing, and bleaching conditions on bacterial cellulose fabric production. *Textile Research Journal, 89*(6), 1094–1104. https://doi.org/10.1177/0040517518763989

Hosseini, H. A., Heydari, S., & Es'haghiZare, Z. L. (2022). Multiparameter optimization of magnetite solid-phase microextraction for preconcentration of diclofenac and determination by UV-Vis spectrophotometry. *Journal of the Iranian Chemical Society, 19*, 1747–1754. https://doi.org/10.1007/s13738-021-02414-6

Jebel, F. S., & Almasi, H. (2016). Morphological, physical, antimicrobial and release properties of ZnO nanoparticles-loaded bacterial cellulose films. *Carbohydrate Polymers, 149*, 8–19. https://doi.org/10.1016/j.carbpol.2016.04.089

Jiamsawat, C., Wasanapiarnpong, T., & Srikulkit, K. (2022). Improving carbon yield of bacterial cellulose derived carbon by phosphorus/nitrogen doping. *Materials Today Communications, 33*, Article 104382. https://doi.org/10.1016/j.mtcomm.2022.104382

Kambli, N. D., Samanta, K. K., Basak, S., Chattopadhyay, S. K., Patil, P. G., & Deshmukh, R. R. (2018). Characterization of the corn husk fibre and improvement in its thermal stability by banana pseudostem sap. *Cellulose, 25*, 5241–5257. https://doi.org/10.1007/s10570-018-1931-z

Kasaai, M. R. (2018). Zein and zein-based nano-materials for food and nutrition applications: A review. *Trends in Food Science & Technology, 79*, 184–197. https://doi.org/10.1016/j.tifs.2018.07.015
Keshk, S., & Sameshima, K. (2006). Influence of lignosulfonate on crystal structure and productivity of bacterial cellulose in a static culture. *Enzyme and Microbial Technology, 40*(1), 4–8. https://doi.org/10.1016/j.enzmictec.2006.07.037
Khatkar, B. S., Barak, S., & Mudgil, D. (2013). Effects of gliadin addition on the rheological, microscopic and thermal characteristics of wheat gluten. *International Journal of Biological Macromolecules, 53*, 38–41. https://doi.org/10.1016/j.ijbiomac.2012.11.002
Kim, H., & Kim, H. R. (2023). Production of flame-resistant bacterial cellulose using whey protein isolate or casein via physical entrapment and crosslinking. *Cellulose, 30*, 9295–9330. https://doi.org/10.1007/s10570-023-05452-w
Kim, H., Song, J. E., & Kim, H. R. (2021a). *Ex situ* coloration of laccase-entrapped bacterial cellulose with natural phenolic dyes. *Journal of the Korean Society of Clothing and Textiles, 45*(5), 866–880. https://doi.org/10.5850/JKSCT.2021.45.5.866
Kim, H., Song, J. E., & Kim, H. R. (2021b). Comparative study on the physical entrapment of soy and mushroom proteins on the durability of bacterial cellulose bio-leather. *Cellulose, 28*, 3183–3200. https://doi.org/10.1007/s10570-021-03705-0
Kim, H., Song, J. E., Silva, C., & Kim, H. R. (2020). Production of conductive bacterial cellulose-polyaniline membranes in the presence of metal salts. *Textile Research Journal, 90*(13–14), 1517–1526. https://doi.org/10.1177/0040517519893717
Kiziltas, E. E., Kiziltas, A., Blumentritt, M., & Gardner, D. J. (2015). Biosynthesis of bacterial cellulose in the presence of different nanoparticles to create novel hybrid materials. *Carbohydrate Polymers, 129*, 148–155. https://doi.org/10.1016/j.carbpol.2015.04.039
Kudo, S., & Nakashima, S. (2020). Changes in IR band areas and band shifts during water adsorption to lecithin and ceramide. *Spectrochimica Acta Part a: Molecular and Biomolecular Spectroscopy, 228*, Article 117779. https://doi.org/10.1016/j.saa.2019.117779
Lee, C. M., Kubicki, J. D., Fan, B., Zhong, L., Jarvis, M. C., & Kim, S. H. (2015). Hydrogen-bonding network and OH stretch vibration of cellulose: Comparison of computational modeling with polarized IR and SFG spectra. *The Journal of Physical Chemistry B, 119*(49), 15138–15149. https://doi.org/10.1021/acs.jpcb.5b08015
Li, Q., Gao, R., Wang, L., Xu, M., Yuan, Y., Ma, L., Wan, Z., & Yang, X. (2020). Nanocomposites of bacterial cellulose nanofibrils and zein nanoparticles for food packaging. *ACS Applied Nano Materials, 3*(3), 2899–2910. https://doi.org/10.1021/acsanm.0c00159
Li, Y.-C., Mannen, S., Morgan, A. B., Chang, S. C., Yang, Y.-H., Condon, B., & Grunlan, J. C. (2011). Intumescent all-polymer multilayer nanocoating capable of extinguishing flame on fabric. *Advanced Materials, 23*(34), 3926–3931. https://doi.org/10.1002/adma.201101871
Lin, S.-B., Hsu, C.-P., Chen, L.-C., & Chen, H.-H. (2009). Adding enzymatically modified gelatin to enhance the rehydration abilities and mechanical properties of bacterial cellulose. *Food Hydrocolloids, 23*(8), 2195–2203. https://doi.org/10.1016/j.foodhyd.2009.05.011
Liu, J., Dunne, F. O., Fan, X., Fu, X., & Zhong, W.-H. (2019). A protein-functionalized microfiber/protein nanofiber Bi-layered air filter with synergistically enhanced filtration performance by a viable method. *Separation and Purification Technology, 229*, Aticle 115837. https://doi.org/10.1016/j.seppur.2019.115837
Liu, J., Wang, Z., Wang, Z., Hao, Y., Wang, Y., Yang, Z., Li, W., & Wang, J. (2020). Physicochemical and functional properties of soluble dietary fiber from different colored quinoa varieties (*Chenopodium quinoa* Willd). *Journal of Cereal Science, 95*, Article 103045. https://doi.org/10.1016/j.jcs.2020.103045
Martelli-Tosi, M., Masson, M. M., Silva, N. C., Esposto, B. S., Barros, T. T., Assis, O. B. G., & Tapia-Blácido, D. R. (2018). Soybean straw nanocellulose produced by enzymatic or acid treatment as a reinforcing filler in soy protein isolate films. *Carbohydrate Polymers, 198*, 61–68. https://doi.org/10.1016/j.carbpol.2018.06.053
Mathew, M. S., Vinod, K., Jayaram, P. S., Jayasree, R. S., & Joseph, K. (2019). Improved bioavailability of curcumin in gliadin-protected gold quantum cluster for targeted delivery. *ACS Omega, 4*(10), 14169–14178. https://doi.org/10.1021/acsomega.9b00917
Mejia, C. D., Mauer, L. J., & Hamaker, B. R. (2007). Similarities and differences in secondary structure of viscoelastic polymers of maize α-zein and wheat gluten proteins. *Journal of Cereal Science, 45*(3), 353–359. https://doi.org/10.1016/j.jcs.2006.09.009
Mohammadia, M., Es'haghi, Z., & Hooshmand, S. (2018). Green and chemical synthesis of zinc oxide nanoparticles and size evaluation by UV-vis spectroscopy. *Journal of Nanomedicine Research, 7*(1), Article 00175. https://doi.org/10.15406/jnmr.2018.07.00175
Nallathambi, G., Ramachandran, T., Rajendran, V., & Palanivelu, R. (2011). Effect of silica nanoparticles and BTCA on physical properties of cotton fabrics. *Materials Research, 14*(4), 552–559. https://doi.org/10.1590/s1516-14392011005000086
Peng, F., Jin, Y., Wang, K., Wang, X., Xiao, Y., & Xu, H. (2022). Glycosylated zein composite nanoparticles for efficient delivery of betulinic acid: Fabrication, characterization, and in vitro release properties. *Foods, 11*(17), Article 2589. https://doi.org/10.3390/foods11172589
Peng, J., Zhu, K.-X., Guo, X.-N., & Zhou, H.-M. (2021). The impact of phosphates on the fibrous structure formation of textured wheat gluten. *Food Hydrocolloids, 119*, Article 106844. https://doi.org/10.1016/j.foodhyd.2021.106844
Peydayesh, M., Bagnani, M., Soon, W. L., & Mezzenga, R. (2023). Turning food protein waste into sustainable technologies. *Chemical Reviews, 123*(5), 2112–2154. https://doi.org/10.1021/acs.chemrev.2c00236
Poletto, M., Zattera, A. J., Forte, M. M. C., & Santana, R. M. C. (2012). Thermal decomposition of wood: Influence of wood components and cellulose crystallite size. *Bioresource Technology, 109*, 148–153. https://doi.org/10.1016/j.biortech.2011.11.122
Rani, M., Sogi, D. S., & Gill, B. S. (2021). Characterization of gliadin, secalin and hordein fractions using analytical techniques. *Scientific Reports, 11*, Article 23135. https://doi.org/10.1038/s41598-021-02099-0
Raza, Z. A., Anwar, F., Hussain, I., Abid, S., Masood, R., & Maqsood, H. S. (2018). Fabrication of PLA incorporated chitosan nanoparticles to create enhanced functional properties of cotton fabric. *Pigment & Resin Technology, 48*(2), 169–177. https://doi.org/10.1108/PRT-11-2017-0088

Sheykhnazari, S., Tabarsa, T., Mashkour, M., Khazaeian, A., & Ghanbari, A. (2018). Multilayer bacterial cellulose/resole nanocomposites: Relationship between structural and electro-thermo-mechanical properties. *International Journal of Biological Macromolecules, 120*, 2115–2122. https://doi.org/10.1016/j.ijbiomac.2018.09.047

Song, J. E., Su, J., Loureiro, A., Martins, M., Cavaco-Paulo, A., Kim, H. R., & Silva, C. (2017). Ultrasound-assisted swelling of bacterial cellulose. *Engineering in Life Sciences, 17*, 1108–1117. https://doi.org/10.1002/elsc.201700085

Tang, X. Z., Kumar, P., Alavi, S., & Sandeep, K. P. (2012). Recent advances in biopolymers and biopolymer-based nanocomposites for food packaging materials. *Critical Reviews in Food Science and Nutrition, 52*(5), 426–442. https://doi.org/10.1080/10408398.2010.500508

Tariq, H., Rehman, A., Kishwar, F., & Raza, Z. A. (2022). Citric acid cross-linking of chitosan encapsulated spearmint oil for antibacterial cellulosic fabric. *Medical Polymers, 64*, 456–466. https://doi.org/10.1134/S0965545X22700158

Villarreal-Soto, S. A., Bouajila, J., Beaufort, S., Bonneaud, D., Souchard, J.-P., & Taillandier, P. (2020). Physicochemical properties of bacterial cellulose obtained from different Kombucha fermentation conditions. *Journal of Vinyl & Additive Technology, 27*(1), 183–190. https://doi.org/10.1002/vnl.21795

Wan, Z., Wang, L., Ma, L., Sun, Y., & Yang, X. (2017). Controlled hydrophobic biosurface of bacterial cellulose nanofibers through self-assembly of natural zein protein. *ACS Biomaterials Science & Engineering, 3*(8), 1595–1604. https://doi.org/10.1021/acsbiomaterials.7b00116

Wang, K., Luo, S., Cai, J., Sun, Q., Zhao, Y., Zhong, X., Jiang, S., & Zheng, Z. (2016). Effects of partial hydrolysis and subsequent cross-linking on wheat gluten physicochemical properties and structure. *Food Chemistry, 197*, 168–174. https://doi.org/10.1016/j.foodchem.2015.10.123

Wang, X., Ullah, N., Sun, X., Guo, Y., Chen, L., Li, Z., & Feng, X. (2017). Development and characterization of bacterial cellulose reinforced biocomposite films based on protein from buckwheat distiller's dried grains. *International Journal of Biological Macromolecules, 96*, 353–360. https://doi.org/10.1016/j.ijbiomac.2016.11.106

Xie, J., Yan, Y., Pan, Q.-N., Shi, W.-Z., Gan, J.-H., Lu, Y., Tao, N.-P., Wang, X.-C., Wang, Y., & Xu, C.-H. (2020). Effect of frozen time on *Ctenopharyngodon idella* surimi: With emphasis on protein denaturation by Tri-step spectroscopy. *Journal of Molecular Structure, 1217*, Article 128421. https://doi.org/10.1016/j.molstruc.2020.128421

Xu, B., Shao, L., Wang, J., Liu, Y., & Qian, L. (2020). Enhancement of the intumescent flame retardant efficiency in polypropylene by synergistic charring effect of a hypophosphite/cyclotetrasiloxane bi-group compound. *Polymer Degradation and Stability, 181*, Article 109281. https://doi.org/10.1016/j.polymdegradstab.2020.109281

Xu, Y., Jia, Z., Wang, J., Sun, J., & Song, R. (2022). Property and stability of astaxanthin emulsion based on pickering emulsion templating with zein and sodium alginate as stabilizer. *International Journal of Molecular Sciences, 23*(16), Article 9386. https://doi.org/10.3390/ijms23169386

Yang, H., Yu, B., Xu, X., Bourbigot, S., Wang, H., & Song, P. (2020). Lignin-derived bio-based flame retardants toward high-performance sustainable polymeric materials. *Green Chemistry, 22*, 2129–2161. https://doi.org/10.1039/d0gc00449a

Yuan, Q., Lu, W., & Pan, Y. (2010). Structure and properties of biodegradable wheat gluten/attapulgite nanocomposite sheets. *Polymer Degradation and Stability, 95*(9), 1581–1587. https://doi.org/10.1016/j.polymdegradstab.2010.06.005

Zhang, S., Jin, X., Gu, X., Chen, C., Li, H., Zhang, Z., & Sun, J. (2018). The preparation of fully bio-based flame retardant poly(lactic acid) composites containing casein). *Journal of Applied Polymer Science, 135*(33), Article 46599. https://doi.org/10.1002/app.46599

If the journal article has an article number instead of a page range, include the word "Article" and then the article number instead of the page range. https://apastyle.apa.org/style-grammar-guidelines/references/examples/journal-article-references#2Zhang, Y., Deng, L., Zhong, H., Zou, Y., Qin, Z., Li, Y., & Zhang, H. (2022). Impact of glycation on physical properties of composite gluten/zein nanofibrous films fabricated by blending electrospinning. *Food Chemistry, 366*, Article 130586. https://doi.org/10.1016/j.foodchem.2021.130586

Zhu, P., Sui, S., Wang, B., Sun, K., & Sun, G. (2004). A study of pyrolysis and pyrolysis products of flame-retardant cotton fabrics by DSC, TGA, and PY-GC-MS. *Journal of Analytical and Applied Pyrolysis, 71*(2), 645–655. https://doi.org/10.1016/j.jaap.2003.09.005

Publisher's Note

Hyunjin Kim Postdoctoral researcher, Korea Institute of Industrial Technology, Ansan-si, Gyeonggi-do, South Korea.

Hye Rim Kim Professor, Sookmyung Women's University, Seoul, South Korea.